

Temperature effects on MIPs in the BGO calorimeters of DAMPE^{*}

Yuan-Peng Wang(王远鹏)^{1,2} Si-Cheng Wen(文思成)^{1,2} Wei Jiang(蒋维)^{1,2} Chuan Yue(岳川)^{1,2}
 Zhi-Yong Zhang(张志永)³ Yi-Feng Wei(魏逸丰)³ YunLong Zhang(张云龙)³
 Jing-Jing Zang(藏京京)^{1,1)} Jian Wu(伍健)¹

¹Key Laboratory of Dark Matter and Space Astronomy, Purple Mountain Observatory, Nanjing 210008, China

²University of Chinese Academy of Sciences, Yuquan Road 19, Beijing 100049, China

³State Key Laboratory of Particle Detection and Electronics, University of Science and Technology of China, Hefei 230026, China

Abstract: In this paper, we present a study of temperature effects on BGO calorimeters using proton MIPs collected in the first year of operation of DAMPE. By directly comparing MIP calibration constants used by the DAMPE data production pipe line, we find an experimental relation between the temperature and signal amplitudes of each BGO bar: a general deviation of $-1.162\%/^{\circ}\text{C}$, and $-0.47\%/^{\circ}\text{C}$ to $-1.60\%/^{\circ}\text{C}$ statistically for each detector element. During 2016, DAMPE's temperature changed by $\sim 8^{\circ}\text{C}$ due to solar elevation angle, and the corresponding energy scale bias is about 9%. By frequent MIP calibration operation, this kind of bias is eliminated to an acceptable value.

Keywords: BGO, MIP, temperature effect

PACS: 29.40.Vj **DOI:** 10.1088/1674-1137/41/10/106001

1 Introduction

The Dark Matter Particle Explorer (DAMPE) is an orbital telescope with high resolution and wide energy band aiming at detecting cosmic rays and gamma-rays of 0.5 GeV – 100 TeV [1–3]. Apart from the supporting structures of the satellite, the telescope itself consists of four sub-detectors. From top to bottom (along the direction towards the center of the Earth) are plastic scintillator detectors (PSD, 82 units), a silicon tungsten tracker (STK, 768 units), bismuth germanate oxide detectors (BGO, 308 units), and neutron detectors (NUD, 4 units), where the number of units means the number of corresponding crystals, for example, there are 308 BGO crystal bars on DAMPE. Each of the four sub-detectors has its own targets: PSD for charge, BGO for energy/PID, STK for direction/charge, and NUD for particle identification. Together, they make DAMPE an orbital telescope with the ability to measure high-energy particles up to 100 TeV with good angular resolution [1].

To measure the parameters above, DAMPE has to deal with thousands of electronic channels that connect the PMTs of physical detectors with the data processor to store the information wanted. Calibration is required

to convert the charge excited by interaction between particles and DAMPE to the energy of the particles. A detailed description of the procedure can be found elsewhere [4], and only part of it is described here: the effects of temperature on the response to MIPs of the BGO calorimeters of DAMPE.

MIPs, short for minimum-ionization particles, whose energy loss in material can be quantified by the Bethe-Block formula, are the kind of particles that can penetrate materials while depositing energy only by ionization rather than suffering nuclear reactions. This means that the energy they lose makes up nearly a fixed percentage of their total energy. Assisted by simulation with the same structure and (nearly) the same energy spectrum (Section 2 below introduces it briefly), the exact energy of a MIP is acquired, and is then utilized to calibrate the BGO and PSD by matching that energy with the magnitude of the ADC (Analog to Digital Conversion²⁾) signal collected by the PMTs when a MIP hits them [5]. A thorough understanding of the particles hitting DAMPE requires much more effort than MIP calibration ("MIP calibration" is used hereafter for "the procedure of calibrating the ADC values of MIPs to acquire their ADCs for future use") alone. For example, the relation between

Received 24 March 2017, Revised 6 July 2017

^{*} This work was supported by National Key Program for Research and Development (No. 2016YFA0400200) and by NSFC (11303105, 11673021). The DAMPE mission was funded by the strategic priority science and technology projects in space science of the Chinese Academy of Sciences (No. XDA04040000 and No. XDA04040400)

1) E-mail: zangjj@pmo.ac.cn

2) In many other cases one may expect "Convertor" instead of "Conversion". Here we use the latter because "ADC" hereafter is used as a unit measuring the charge rather than the convertor itself.

©2017 Chinese Physical Society and the Institute of High Energy Physics of the Chinese Academy of Sciences and the Institute of Modern Physics of the Chinese Academy of Sciences and IOP Publishing Ltd

different dynodes of a PMT should also be calibrated, which can also be found in Ref. [5].

However, the magnitude of charge read from a PMT when a particle hits BGO is actually determined not only by the nature of that particle but also by the PMT itself [6]. So the environment of the PMTs will affect their behavior. Temperature is one of the most important factors which is affected by the angle of the satellite, as it gets heated by sunshine. A previous experimental estimation [7] tells us that its influence on the behavior of PMTs is approximately $-1\%/^{\circ}\text{C}$, but the precision of that estimation was far from acceptable. So this paper aims at a more accurate evaluation of this effect by comparing the data from DAMPE from about one year, covering a range of temperature of $2\text{--}10^{\circ}\text{C}$. After the comparison, a linear fit is applied, allowing more precise evaluation of this effect.

Simulation is used in many parts of our analysis, and this paper introduces it briefly in the next section, followed by our procedure for selecting MIP samples and a brief fitting result. After that is the major topic, the temperature effects of MIPs, which is arranged in three parts: the variation of temperature and MIP results on different dates, the global relation between temperature and MIP calibration constants, and finally the results of each BGO calorimeter. Finally we come to the conclusion.

2 The DAMPE simulation

A detailed description of simulation in DAMPE is in preparation, and here only a brief introduction is given, with special attention paid to MIPs.

DAMPE uses GEANT4 as the basis for simulation [8, 9]. First we take the spectrum from AMS02 as the input of GEANT4. Now the energy of MIPs is affected by the angular distribution, so DAMPE's orbit must be taken. A technique called "back-tracing" is therefore applied to target the particles according to the orbital parameters of DAMPE (time and position). This technique enables a particle in GEANT4 to swirl in a magnetic field according to the geomagnetic field at the same coordinates as DAMPE when it is being considered, so we can then re-model the spectrum for DAMPE. Because the tracks of particles coming from earth will eventually collide with the earth if we reverse-extend them, abandoning these particles offers us a fine spectrum with orbital information of DAMPE. The difference between the real spectrum and that from our simulation is quite acceptable, as can be seen from Ref. [10].

With simulation data, we can find perfect MIP samples whose exact energy is known from input. Using a digitization technique, the ADCs of the MIPs are also provided. These values are used as defaults, for example

in the case of a new environment where no calibration for MIPs is available, considering they are independent of real data. Later in the following analysis, they are also used as a reference to give a normalized relation where the real values are not concerned.

3 Procedure for selecting MIPs

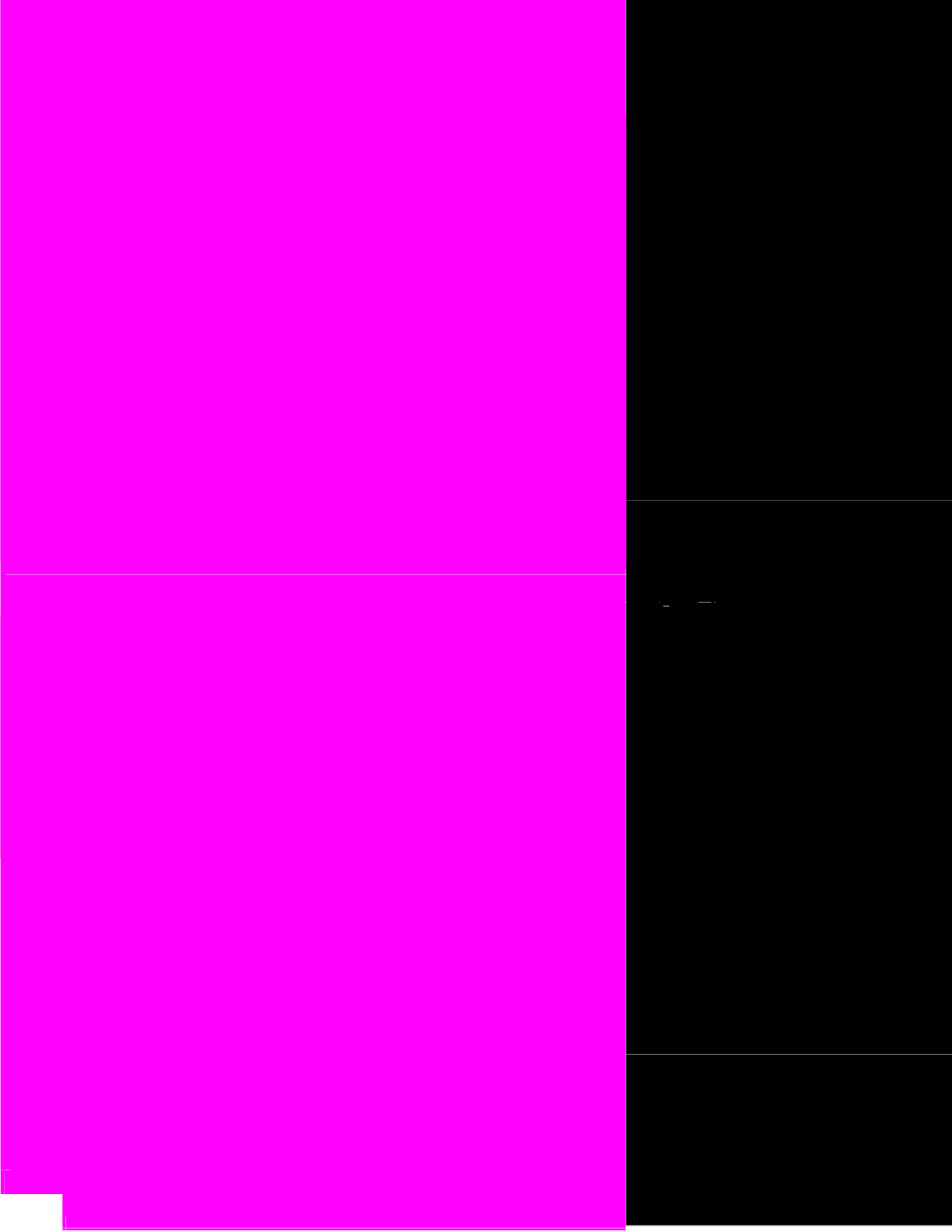
MIPs are defined, in this work, as particles which lose energy only by electromagnetic reactions with materials. Consequently, the ratio of MIPs when penetrating materials is determined by the geometric structure and the materials themselves. Apart from ionization energy loss, MIPs hardly interact with materials, making their track quite straight and clear when penetrating DAMPE. These facts pave the way for determining whether a particle can contribute to MIP calibration. Five different filters for MIPs have been developed accordingly and are listed below. Of these, one specific filter is designed only for DAMPE. All filters below are listed in the order they are arranged in the code. If one filter rejects a particle when it is being checked, it will be thrown away immediately without checking the rest of the filters. Reference [11] details the software framework we use.

1) Trigger mode

Exposed directly to cosmic rays, DAMPE gets hit by millions of particles every minute, the majority of which are low-energy and thus low priority. This makes the data selection procedure extremely important. The trigger mode of DAMPE decides what to record. Several trigger modes are designed for DAMPE because it has many scientific tasks. Some modes are designed to increase the number of MIPs due to their significance in calibration. In this way, selecting certain trigger modes can help preclude a large number of particles when only MIPs are needed. MIP modes are enabled only at low latitudes ($20^{\circ}\text{S}\text{--}20^{\circ}\text{N}$). Details of the DAMPE trigger system are available elsewhere. This is a DAMPE-specific filter.

2) Penetration

This filter, making sure that a particle has deposited energy in both the top and bottom of the BGO calorimeter, aims at selecting MIPs that penetrate DAMPE thoroughly by throwing away those entering or leaving DAMPE through one side of this satellite. It is currently a compromise to sacrifice the efficiency of MIP selection for the sake of energy estimation, because otherwise the ratio of the energy from the BGO calorimeter to that of the particle cannot be easily decided, making it impossible to acquire a good evaluation of the energy of the particle. Now that the energy spectrum of MIP is necessary when calibrating, these "crippled" MIPs are



points makes it difficult to plot them all on the same figure, so there are four individual diagrams. We will come back to real ADCs when linearity is concerned. Also, the MPV from the fitting function of the ADCs is plotted each time, and vertical axes are thus labeled accordingly.

Here the MPVs of each bar fluctuate more than in the global case. We find two reasons for this. Firstly, the global relation stated above is concluded by a statistical study of 308 bars where individual deviations are largely tolerated. Secondly, this can be understood by the fitting procedure. Fitting relies on the initial values of each parameter. This dependency dominates in the case of the convolution of a Landau and Gaussian function, where a minor deviation in the initial value may lead to visible mismatch, and MIP calibration depends on this convolution. Initially, recursive efforts were made to improve the initial conditions as well as the fitting range for better results, then a two-phase fitting process was developed, where the first trial aims only at providing the initial conditions for the real fitting in the second phase. In doing this, only the MPV of the first trial is

used to construct the initial conditions for the second fitting. We use only MPV, which can be roughly estimated as the peak of the data, because not too many steps are needed to acquire this parameter, because of efficiency, and because it is observed that the MPV is still reliable even if the fitting fails. This two-phase fitting method recovers many failures from the previous fitting method because the new initial conditions it uses are more reasonable. If the reduced $\chi^2 (= \chi^2/NDF)$ is larger than 3, we consider this two-phase fitting to have failed as well, and then a third fit is performed. For this third trial, the MPV of the second fit is still consulted to give the initial conditions but in a slightly different way than that in the second trial to avoid further failure, and these differences also come from our recursive trial. In other words, each histogram is fitted at least twice but at most three times, and these efforts give us the smoothness in fitting functions like Fig. 1 with few exceptions in the end.

The final part is linearity of temperature and MIPs, shown for four bars in Fig. 6. A statistical analysis for all the bars is shown in Fig. 7 and 8.

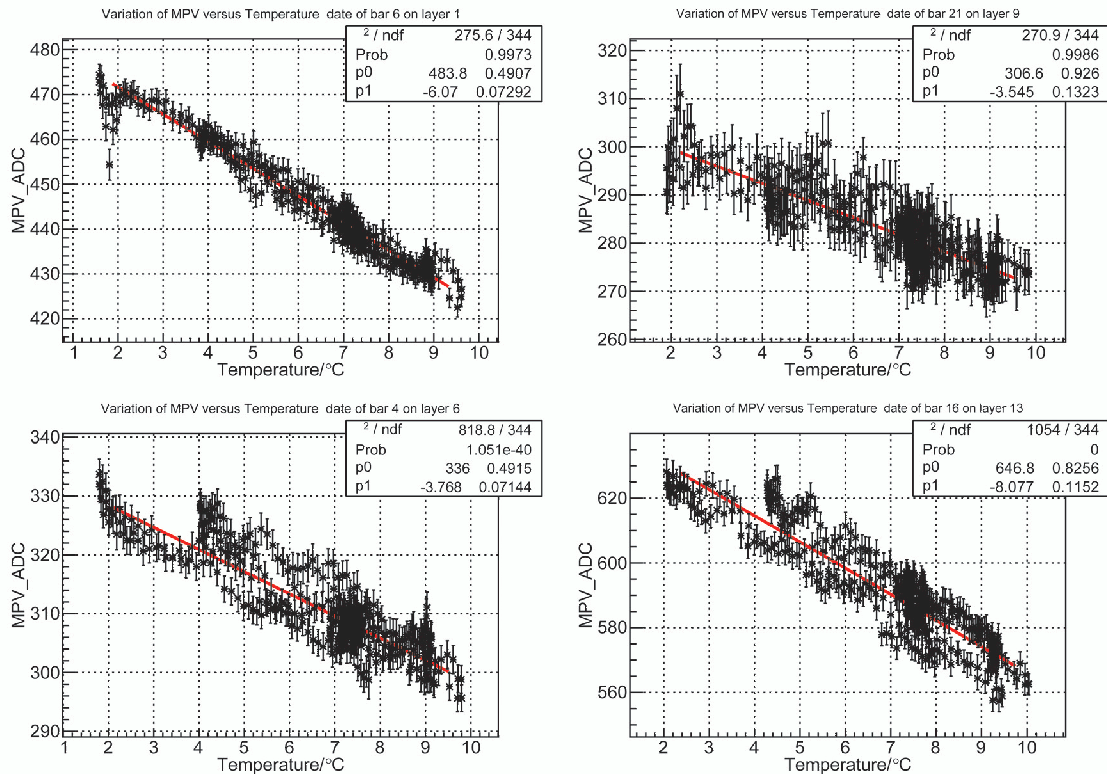


Fig. 6. (color online) Relation between temperature and MIP constants of the same 4 BGO bars as chosen above.

The top two diagrams show good linearity while the bottom two are less good. The relation here deviates from linearity due to the relatively large deviation of MPVs of MIPs of each bar as displayed and explained in the text. It remains true, however, that higher temperature brings about lower MIPs. As in the global case, not all the data points are used, and the ranges here correspond with 2–9°C in the global case (see the text).

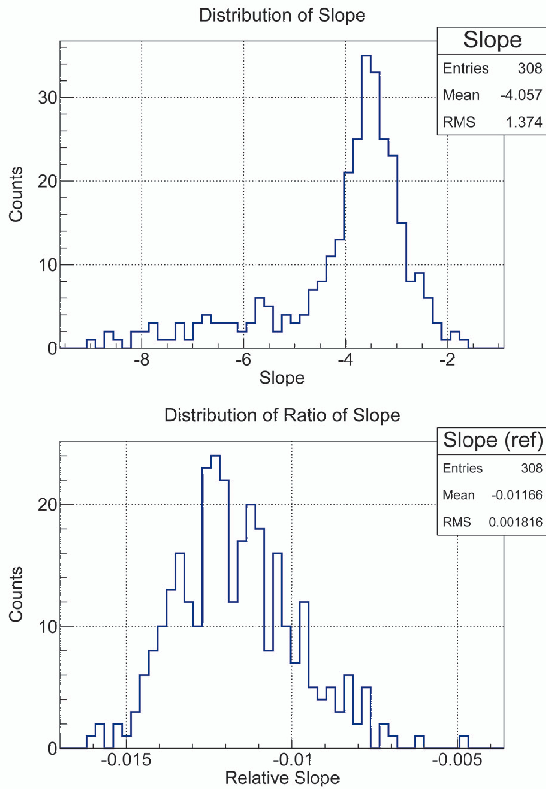


Fig. 7. (color online) Distribution of slopes of linearity between temperature and MIP constants of 308 BGO bars. All slopes are negative. (a) The absolute values, calculated directly by linearly fitting the MIP constants and temperature instead of a ratio. (b) The relative values, or ratio of the value of each bar to that acquired by simulation results. The average ratio is -1.16% , which matches the global result well.

Following the restricted range, the first step is find the corresponding range for each unit. $2-9^{\circ}\text{C}$ is not suitable here because thermal equilibrium does not mean

that all bars share the same temperature. It is possible to calculate using linear interpolation, provided that the same tendency holds for all bars with minor deviation, as mentioned before. It is an easy method with good resolution, much easier than the most reliable way which requires a thorough calculation for either condition. From these figures one can also obtain a standard for selecting bars: normal bars with good linearity (such as the Fig. 6(a) and (b), $\sim 83\%$ in all bars), and abnormal bars with bad linearity (such as the Fig. 6(c) and (d) $\sim 17\%$) where good linearity means a bar with a fitting function whose $\chi^2/NDF < 1.19$ (this "1.19" is actually an empirical standard which we set by using a typical ambiguous bar from early analysis). A closer look at those abnormal bars gives another hint: they are usually located on or near the edge of the 308 BGO units of DAMPE¹⁾. It may explain their behavior to understand the lack of statistics compared with the rest. However abnormal a bar appears, their slopes are always negative.

Figures 7 and 8 show the distribution of fitting parameters, where a "ref" in the title (short for "reference") means that the values inserted have been divided by those from simulation.

The absolute value of the average of slopes in Fig. 7(a), -4.057 , is very large compared to the other figure where values have been divided. This direct insertion of slope looks quite loose and is less statistically important than Fig. 7(b). The values in Fig. 7(b) have been divided by simulation results. It gives a mean relative slope of -0.01166 , indicating an average temperature effect of about $-1.166\%/^{\circ}\text{C}$, in accordance with the global result -1.162% presented above. The behavior of different BGO bars varies from $-0.47\%/^{\circ}\text{C}$ to $-1.60\%/^{\circ}\text{C}$. If this effect were ignored, the energy resolution would definitely suffer: considering the temperature change of about 8°C , ignoring temperature would induce a deviation in energy of about 9% .

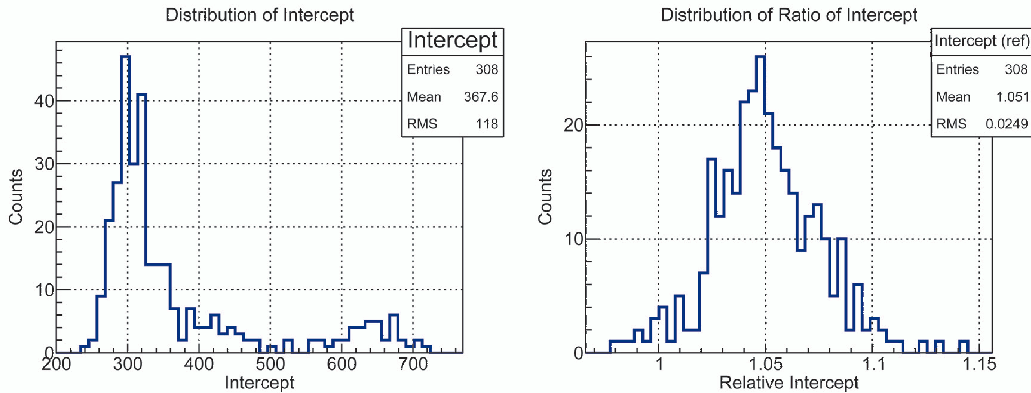


Fig. 8. (color online) Distribution of intercepts.

1) All 308 BGO bars are arranged in 14 layers of 22 BGO bars each. The index of bars, either of its layer or its bar, starts with 0, for example, layer 0 bar 0 is the first bar, layer 8 bar 10 gives the 11th bar on layer 9, and so on.

For completeness, the distribution of intercepts is displayed in Fig. 8. The mean of the relative intercept, 1.051, is in accordance with the global mean in Fig. 4.

5 Conclusion

Data from DAMPE has been used to calibrate MIPs for its BGO detectors. Thermistors uniformly installed in DAMPE enable us to estimate its temperature field. Combination of the calibration results with the temperature field makes it possible to analyze the temperature effects on MIPs of BGO bars (as well as PMTs).

This analysis has been done not only on DAMPE as a whole to analyze the global behavior, but also on each of its 308 BGO bars. The global analysis gives a temperature effect of $-1.162\%/^{\circ}\text{C}$, which means that every degree Celsius brings about a global deviation of -1.162% to the behavior of DAMPE's BGO calorimeters. In terms of one bar alone, the average of all 308

bars gives -1.166% , and individual behavior differs from one bar to another from $-0.47\%/^{\circ}\text{C}$ to $-1.60\%/^{\circ}\text{C}$. From Fig. 2, there have been changes in temperature of $\sim 8^{\circ}\text{C}$ since the launch of DAMPE, which would have introduced a global energy bias of $\sim 9\%$ on DAMPE if the temperature effect was ignored, and would be even worse for individual BGO bars.

The authors sincerely thank the whole DAMPE collaboration, without whom it would be completely impossible to perform this analysis. We especially thank Prof Jin Chang, the chief scientist of DAMPE, who established this project and had gathered this team. We also thank Prof Ming-Sheng Cai and his DAMPE payload group for offering us an excellent detector system. We also thank the Scientific Application System for providing us with reliably reconstructed flight data. All diagrams have been plotted with ROOT (<https://root.cern.ch/>).

References

- 1 J. Chang, Chin. J. Spac. Sci., **34**(5): 550–557 (2014)
- 2 J. Chang, L. Feng, J. Guo et al, Scientia Sinica Physica, Mechanica Astronomica, **45**(11): 119510 (2015) (in Chinese)
- 3 J. Chang and C. DAMPE, arXiv:1706.08453, 2017
- 4 Y. Zhang, B. Li, and C. Feng, Chinese Physics C, **36**: 71 (2012)
- 5 Z. Zhang, C. Wang, J. Dong, and Y. Wei, Nucl. Instrum. Methods Phys. Res., **836**: 98–104, (2016)
- 6 Y. Hu, J. Chang, D. Chen, J. Guo, Y. Zhang, and C. Feng, Chinese Physics C, **40**(11): 116003 (2016)
- 7 Y. Wei, Z. Zhang, Y. Zhang, and S. Wen, Journal of Instrumentation, **11**(7): T07003 (2016)
- 8 S. Agostinelli, Nuclear Instruments and Methods in Physics Research A, **506**: 250–303 (2003)
- 9 J. Allison, Nuclear Instruments and Methods in Physics Research A, **835**: 186–225 (2016)
- 10 C. Yue, J. Zang, T. Dong, X. Li, Z. Zhang, Z. Stephan, J. Wei, Y. Zhang, and D. Wei, Nuclear Instruments and Methods in Physics Research Section A, **856**: 11–16 (2017)
- 11 C. Wang, D. Liu, Y. Wei, Z. Zhang, Y. Zhang, X. Wang, and Xu Zizong, arXiv:1604.03219, 2016